

Multiwavelength study of the starburst galaxy NGC 7714. I: Ultraviolet-Optical spectroscopy¹

Rosa M. González Delgado

Instituto de Astrofísica de Andalucía, Apdo. 3004, 18080 Granada, Spain

Space Telescope Science Institute, 3700 San Martin Drive, Baltimore, MD 21218

Electronic mail: rosa@iaa.es, gonzalez@stsci.edu

María Luisa García-Vargas

GTC-project. Instituto de Astrofísica de Canarias, Vía Lactea, S/N, 38200 La Laguna, Tenerife, Spain

Electronic mail: mgarcia@iac.es

Jeff Goldader

Space Telescope Science Institute, 3700 San Martin Drive, Baltimore, MD 21218

Electronic mail: goldader@stsci.edu

Claus Leitherer

Space Telescope Science Institute, 3700 San Martin Drive, Baltimore, MD 21218

Electronic mail: leitherer@stsci.edu

Anna Pasquali

ST-ECF/ESO, Karl-Schwarzschild-Strasse 2, D-85748 Garching bei Muenchen, Germany

Electronic mail: apasqual@eso.org

¹ Based on observations with the NASA/ESA Hubble Space Telescope obtained at the Space Telescope Science Institute, which is operated by AURA, Inc., under NASA contract NAS5-26555.

ABSTRACT

We have studied the physical conditions in the central 300 pc of the proto-typical starburst galaxy NGC 7714. Our analysis is based on ultraviolet spectroscopy with the HST+GHRS and ground-based optical observations, and it covers also X-ray and radio data taken from the literature. The data are interpreted using evolutionary models optimized for young starburst regions. The massive stellar population is derived in a self-consistent way using the continuum and *stellar* absorption lines in the ultraviolet and the *nebular* emission line optical spectrum.

The central starburst has an age of about 4.5 Myr, with little evidence for an age spread. Wolf-Rayet features at the ultraviolet indicates a stellar population of ~ 2000 Wolf-Rayet stars. The overall properties of the newly formed stars are quite similar to those derived, e.g., in 30 Doradus. A standard Salpeter IMF is consistent with all observational constraints. The nucleus of NGC 7714 has a bolometric luminosity of $0.5\text{--}1 \times 10^{10} L_{\odot}$ and a mass of $5\text{--}10 \times 10^6 M_{\odot}$ (if low-mass stars have formed). We find evidence for spatial structure within the central 300 pc sampled. Therefore it is unlikely that the nucleus of NGC 7714 hosts a single star cluster exceeding the properties of other known clusters. Contrary to previous suggestions, we find no evidence for a nuclear supernova rate that would significantly exceed the total disk-integrated rate. About one supernova event per century is predicted. Most of them are associated with the core-collapse of a hydrogen-free or -poor progenitor. An older stellar generation, with ages of tens of Myr and older, is suggested as well. This population is less concentrated towards the nucleus and extends over kpc scales

Subject headings: galaxies:evolution–galaxies:starburst–galaxies:stellar content–galaxies:ultraviolet–galaxies:ISM–stars:early-type–galaxies:individual:NGC 7714.

1. Introduction: NGC 7714 a test case for evolutionary synthesis models

Starburst galaxies are objects in which the total energetics are dominated by star formation and associated phenomena (Weedman 1983; Heckman 1998). This definition covers galaxies with a very wide range of properties, from blue compact dwarfs to ultraluminous IRAS starbursts. Typical masses (bolometric luminosities) range from 10^6 to $10^{10} M_{\odot}$ (10^9 to $10^{14} L_{\odot}$), corresponding the lowest limit to the mass of super-star-clusters and the highest limit to the mass of the infrared-luminous galaxies (Leitherer 1996). Nearby starburst galaxies are ideal laboratories in which to explore fundamental questions about the local and global processes and effects of star formation. For example, is the initial mass function the same in starburst galaxies as in quiescent star formation in the Milky Way? Is there a connection between starburst activity and active galactic nuclei? What can starbursts teach us about the process by which the first galaxies formed?

Starburst are powered by massive stars. Massive stars ($M \geq 10 M_{\odot}$) emit photons with energies of tens of eV which are absorbed and re-emitted in their stellar winds, producing ultraviolet resonance transitions. However, the stellar wind is optically thin to most of the ultraviolet photons, that can travel tens of pc from the star before they are absorbed and photoionize the surrounding interstellar medium. Then, this ionized gas cools down via an emission line spectrum. This is, in essence, the spectral dichotomy picture of a starburst galaxy: a nebular emission line spectrum at optical wavelengths and an absorption-line spectrum at wavelengths shorter than the Balmer jump (Leitherer 1997). However, the presence of a starburst affects the entire spectrum and not only the UV-optical spectrum. Thus, supernova remnants following the explosion of massive stars generate X-ray and radio continuum emission; red supergiant stars emit strongly in the near-IR continuum; the mid-IR is dominated by line and continuum emission from warm dust within the star forming regions; the far-IR is thermal emission from dust heated by absorbing UV and optical light; electron accelerated by supernova remnants create radio synchrotron emission. A truly complete analysis of a starburst would account for all these features.

Evolutionary synthesis is a powerful tool for understanding starburst galaxies. This technique makes a

prediction for the spectrum of a stellar population taking as a free parameter the star formation history of the starburst (age, initial mass function, star formation rate, etc). If there is agreement between the observations and the predicted physical properties (spectral energy distribution, colors, line profiles, etc), constraints on the star formation history (in timescale between 1 Myr to several Gyr) can be determined (see e.g. Mas-Hesse & Kunth, 1991; Bruzual & Charlot, 1993; Leitherer & Heckman, 1995). However, the solution obtained with this technique may not be unique, and only *consistency* between models and observations can be derived.

To make a complete analysis of a starburst, we have to answer the question: are evolutionary synthesis models, and the stellar evolution models they incorporate, actually up to the challenge of interpreting multi-wavelength data? To answer this, we have undertaken a detailed study of the starburst galaxy NGC 7714.

NGC 7714 is an SBb peculiar galaxy (de Vaucouleurs et al 1991) classified by Weedman et al (1981; here after W81) as a prototypical starburst galaxy. Its heliocentric radial velocity, as compiled by NASA Extragalactic Database (NED), is 2798 km s^{-1} . This places NGC 7714 at a distance of 37.3 Mpc assuming $H_0 = 75 \text{ km s}^{-1} \text{ Mpc}^{-1}$. Heckman et al (1998) derive a distance of 37.9 Mpc using the standard linear Virgo centric infall model of Schechter (1980) with parameters $\gamma=2$, $v_{\text{Virgo}} = 976 \text{ km s}^{-1}$, $w_{\odot} = 220 \text{ km s}^{-1}$ and $D_{\text{Virgo}} = 15.9 \text{ Mpc}$. The B magnitude and far-infrared luminosity (as calculated from the $60 \mu\text{m}$ and $100 \mu\text{m}$ IRAS bands) are -20.04 and 43.93 erg s^{-1} , respectively. The far-infrared ratio $60/100$ and $25/60$ are larger than 0.9 and 0.25 , respectively. The mass of the neutral gas is $\sim 10^{10} M_{\odot}$ (Mirabel & Wilson, 1989). The X-ray, IUE ultraviolet, optical, and VLA radio fluxes are explained as a consequence of intense star formation activity in its nucleus. To explain the X-ray and radio luminosities, 10^4 supernova remnants are required (W81). Bernlöhr (1993) found from the optical continuum and FIR colors that the star formation in NGC 7714 is consistent with a continuous star formation rate during the past 20 Myr, and that it had probably been triggered by the interaction with the companion galaxy NGC 7715 (Vorontsov-Velyaminov 1977; Arp 1966; Smith, Struck, & Pogge, 1997). Very detailed studies have been carried out in the optical and near-IR part of the spectrum to characterize the gas properties in the nuclear and circum-

nuclear regions (González-Delgado et al 1995, hereafter GD95, and references therein). GD95 conclude that the burst of star formation in the nucleus of the galaxy should have an age around 4-5 Myr, in view of the WR bump detection, and pointed out the presence of a previous burst of star formation on the basis of the detection of calcium triplet absorption at 8600 Å. Models by García-Vargas et al (1997) indicate that a young burst of age between 3.5 and 5 Myr is able to explain the emission line spectrum and the WR luminosity bump in three circumnuclear HII regions of NGC 7714.

Here, we present HST+GHRS ultraviolet spectroscopy of the nuclear starburst. These data are analyzed together with the optical emission line spectrum to obtain information about the ionizing stellar population. The goal is to perform a consistency test between the stellar content derived from multi-wavelength observations in the central few hundred parsecs in NGC 7714. We will evaluate whether the youngest burst can account for the high supernova rate (1 yr^{-1} ; W81) derived from the X-ray and radio continuum emission. A following paper will present the results for the NIR K-band spectroscopy and the analysis of the multiwavelength spectral energy distribution (SED) (Goldader et al 1998; in preparation). It will focus on the extincted and low mass stellar content of the nuclear starburst in NGC 7714. Calzetti (1997) analyzed the properties of the NGC 7714 starburst on a kpc scale. The new GHRS data allow us to probe the nuclear starburst on a scale that is an order of magnitude smaller. The new data are useful to study if and how the star formation properties in NGC 7714 differ between pc and kpc scales.

The paper is organized as follows. Section 2 presents the HST observations. Section 3 deals with the results and interpretation of the HST ultraviolet spectrum. In Section 4 we present photoionization models that fit the emission line spectrum in the optical-near infrared spectral range. The multiwavelength analysis of the NGC 7714 spectrum is in Section 5. The summary and the conclusions are in Section 6.

2. HST Observations

The ultraviolet spectrum of the central nuclear starburst in NGC 7714 was obtained in October 1996 with the Hubble Space Telescope using the GHRS and the grating G140L, through the Large Science

Aperture (LSA, $1.74 \times 1.74 \text{ arcsec}^2$ corresponding to $330 \times 330 \text{ pc}^2$). Two different wavelength settings were observed, covering 1175 to 1461 Å and 1402 to 1689 Å, with a total integration time of 1659 s and 4542 s, respectively. After standard pipeline processing, the spectra were combined into a single spectrum covering 1175 to 1689 Å, and rebinned to 0.57 Å/pixel, which is the nominal dispersion of the grating. The spectrum was corrected for redshift assuming a radial velocity of 2800 km s^{-1} (GD95). Figure 1 shows the spectrum in the restframe wavelength system of the galaxy.

The spectrum is rich in stellar (CIV $\lambda 1550$, SV $\lambda 1501$, CIII $\lambda 1417$, SiIV $\lambda 1400$, NV $\lambda 1240$, CIII $\lambda 1175$), and interstellar (AlII $\lambda 1670$, FeII $\lambda 1608$, CIV $\lambda 1550$, SiII $\lambda 1527$, SiIV $\lambda 1400$, CII $\lambda 1335$, OI+SiII $\lambda 1302$, SiII $\lambda 1260$) absorption lines. It also shows $\text{L}\alpha$ and HeII $\lambda 1640$ in emission.

Some of the interstellar lines have weaker satellites formed in the Milky Way halo (SiII $\lambda 1527$, SiIV $\lambda 1400$, CII $\lambda 1335$, OI+SiII $\lambda 1302$, and SiII $\lambda 1260$). The zero point of the wavelength calibration was checked by fitting gaussians to the Galactic absorption lines. These lines are blueshifted about 0.3-0.4 Å with respect to the nominal zero point of -2800 km s^{-1} . This is well within the uncertainties expected for an observation through the LSA. The instrumental spectral resolution for a point source within the LSA is about 0.8 Å, but for an extended source it depends on the size of the ultraviolet source. The widths (FWHM) of the gaussians fitted to the Galactic lines are 3.3 Å or 740 km s^{-1} at 1400 Å. This suggests that the object fills a substantial fraction of the aperture.

The flux measured at 1500 Å is $1.9 \times 10^{-14} \text{ erg s}^{-1} \text{ cm}^{-2} \text{ Å}^{-1}$. This is a factor of 2 lower than the IUE flux reported by Kinney et al (1993), indicating that the UV bright stellar population significantly exceeds the area of the GHRS LSA. An HST WFPC2 PC image through the filter F606W ($\lambda_0 = 6010.6 \text{ Å}$, $\Delta\lambda = 1497 \text{ Å}$) was retrieved from the HST archive. The band pass of this filter includes strong emission lines such as [OIII] $\lambda 5007$ and $\text{H}\alpha$, so that the light detected through this filter is not only continuum emission. The integration time was 500 s. The sampling is 0.046 arcsec/pixel, corresponding to 8.7 pc/pixel. Figure 2a shows a view of the whole galaxy. Most of the emission comes from the nucleus with some contribution from the two spiral arms. This central emission is resolved into a compact knot surrounded by several smaller knots. The GHRS spectroscopy

suggests that the starburst is extended at ultraviolet wavelengths as well. Therefore the spatial morphology in the optical and the ultraviolet is rather similar.

3. Stellar content in the nuclear starburst in NGC7714: fitting the HST UV spectrum

3.1. Wind absorption lines

Massive hot stars develop strong stellar winds due to radiation pressure in ultraviolet resonance lines (Morton 1967; Lucy & Solomon 1970). Typical wind velocities in O stars are about 2000 km s^{-1} to 3000 km s^{-1} (Groenewegen, Lamers, & Pauldrach 1989; Prinja, Barlow, & Howarth 1990). As a result, all strong ultraviolet lines in the spectra of O stars originate predominantly in the outflow, and have blueshifted absorptions. The profile shapes reflect the stellar mass-loss rates, which are a strong function of the stellar luminosity (Castor, Abbott, & Klein 1975). Since there exists a well-defined stellar mass-luminosity relation, the line profiles ultimately depend on the stellar mass, and — for a stellar population — on the IMF and SF history (Leitherer, Robert, & Heckman 1995).

The strongest stellar wind resonance features are OVI $\lambda 1034$, NV $\lambda 1240$, SiIV $\lambda 1400$ and CIV $\lambda 1550$. In massive stars, these lines form above the photosphere in the stellar wind — either as a blueshifted absorption in stars with weak winds, or as a P Cygni profile if the wind density is sufficiently high. OVI and CIV are strong lines in O stars of all luminosity classes (Walborn, Bohlin, & Panek 1985; González Delgado, Leitherer, & Heckman 1997). In contrast, SiIV is luminosity dependent, and only blue supergiant stars produce a strong P Cygni profile (Walborn et al 1985). The recombination line HeII $\lambda 1640$ can also be formed in very massive O and WR stars with very dense winds. Evolutionary synthesis models for CIV (Leitherer, Robert, & Heckman 1995) show that the line strength increases for a shallower IMF. The most massive stars are the dominant contributors to the lines, and increasing their numbers relative to the less massive stars which produce the continuum — either via flattening the IMF slope or increasing the upper cut-off mass — leads to stronger lines. SiIV shows a critical dependence on the age of the burst. This spectroscopic method is only efficient in regions of recent star formation activity and high stellar density where the highest masses can be sampled. The technique has been successfully applied to starburst

galaxies (Conti, Leitherer, & Vacca 1996; Leitherer et al 1996; González Delgado et al 1998a) and Seyfert galaxies (Heckman et al 1997; González Delgado et al 1998b). In all these cases, the method has constrained the age and the mass spectrum of the young population.

NGC 7714 has been observed previously by IUE (W81; Kinney et al 1993). The spectra show strong CIV and SiIV in absorption, indicating the presence of massive stars in NGC 7714. However, the interstellar lines are also very strong in NGC 7714 and contribute significantly to the strength of the CIV and SiIV lines. The interstellar contribution can sometimes dominate the profile of the line, as is the case of NGC 1705 (Heckman & Leitherer 1997). This is why an analysis based only in the equivalent width of these lines cannot predict correctly the stellar content and the star formation history of the starburst. To fully resolve the stellar from the interstellar contribution, a resolution better than the IUE resolution of $R=1000$ is required.

The most conspicuous stellar lines in the GHRS spectra of NGC 7714 are the wind lines HeII, CIV, SiIV and NV. We use line profile synthesis of the ultraviolet wind lines to derive the stellar content and to constrain the star formation history of the nuclear starburst. We do not fit the entire line profile of the CIV and SiIV due to the contribution of the interstellar lines, which are not fully accounted for in the models, and are stronger in the starburst spectra than in the synthetic models. We select two windows, corresponding to the blue side of the wind profile ($1381.75\text{--}1390.75 \text{ \AA}$ for SiIV and $1528.0\text{--}1543.75 \text{ \AA}$ for CIV) and to the red side ($1403.5\text{--}1409.5 \text{ \AA}$ for SiIV and $1552.0\text{--}1560.25 \text{ \AA}$ for CIV), where the profile is dominated by the stellar contribution. Then, we compute the χ^2 parameter between the observations and models. The results for SiIV are plotted for burst and continuous star formation (csf) models as a function of the age, upper mass cut-off, and slope of the IMF in Figures 3a,b and 3c,d, respectively. The minimum χ^2 values for SiIV are obtained for instantaneous burst models and a Salpeter IMF. The fit for SiIV requires the presence of O supergiant stars, which appear between 3 and 6 Myr after the burst onset. The best fit is obtained for a 5 Myr burst. The most massive stars present in the starburst have at least a mass of $40 M_{\odot}$. However, we cannot constrain the upper mass cut-off because stars more massive than $40 M_{\odot}$ have already reached the supernova phase at 5 Myr.

Thus, the upper mass cut-off is higher than $40 M_{\odot}$. Figure 4 shows the profiles of the observed CIV and SiIV and the 5 Myr burst model (Salpeter IMF and $M_{up}=100 M_{\odot}$). The CIV profile is equally well fitted by csf models, but it is not possible to constrain the age with these models.

Note that the emission of the NV P Cygni profile is weaker than predicted by the 5 Myr burst model. This discrepancy could be due to the SiII $\lambda 1260$ absorption line formed in the Milky Way halo that falls on the blue edge of the emission part of the profile.

The determination of the age is also consistent with the presence of WR stars in the starburst. WR features have been detected at optical wavelengths (van Breugel et al 1985; GD95), and also in our ultraviolet spectrum. The HeII $\lambda 1640$ is a recombination line which shows a broad emission profile if it is formed in the very dense stellar winds of WR stars and O3-O5 supergiants (Walborn, Bohlin, & Panek 1985). This line is prominent in the GHRS spectrum, and the observed flux is $4 \times 10^{-14} \text{ erg s}^{-1} \text{ cm}^{-2}$. Later we will use this flux to estimate the number of WR stars present in the nuclear starburst.

3.2. Photospheric absorption lines

The spectrum shows several photospheric lines, such as SV $\lambda 1501$, CIII $\lambda 1427$, and SiIII $\lambda 1417$. These lines are prominent in O and early B stars (Walborn et al 1985; Walborn, Parker, & Nichols 1995); they are not resonance lines, and therefore they do not form in the interstellar medium. Their measured equivalent widths are in Table 1. Note that the strength of these lines is also consistent with the synthetic model (see Figure 5).

3.3. Extinction Estimates

To derive the number of WR and O stars in the starburst, we need to estimate the extinction. This can be done using the ultraviolet continuum flux distribution. Leitherer & Heckman (1995) have derived from evolutionary synthesis models that the UV energy distribution arising from a starburst has a spectral index, α , in the range -2.6 to -2.2 ($F_{\lambda} \propto \lambda^{\alpha}$), if the burst is less than 10 Myr old. This spectral index is rather independent of the metallicity and IMF. Therefore, any deviation from the predicted spectral index can be attributed to reddening.

First, the spectrum is corrected for the Galactic extinction, which we derive assuming a ratio of

$N_{HI}/E(B-V) = 4.93 \times 10^{21} \text{ cm}^2$ (Bohlin 1975) and an HI column density towards NGC 7714 of $4 \times 10^{20} \text{ cm}^{-2}$ (Stark et al 1992). The color excess derived is $E(B-V) = 0.08$; this implies an extinction of 0.65 mag at 1500 Å. The slope measured in the corrected spectrum ($\log F_{\lambda}$ vs. $\log \lambda$) after applying the correction for foreground extinction is $\beta = -2.45$, very close to the theoretical value of -2.5 which corresponds to the age deduced from the fit to the absorption profiles. This indicates very low additional internal extinction associated with the starburst. Using the empirical extinction law from Calzetti, Kinney, & Storchi-Bergmann (1994) to match the slope $\beta = -2.45$ to the expected slope $\beta = -2.5$ at 5 Myr, we derive an internal extinction in the starburst of $E(B-V) = 0.03$ (0.26 mag at 1500 Å). The spectrum corrected for total extinction matches the slope of the synthetic spectrum that fits the wind absorption lines (see Figure 5). We note that the total extinction derived from the ultraviolet continuum is lower than the total extinction derived from the Balmer decrement, $E(B-V) = 0.21$ (GD95). This discrepancy between the extinction values derived from the two methods has previously been found by Fanelli, O'Connell, & Thuan (1988) and Calzetti, Kinney, & Storchi-Bergmann (1994). This result suggests that probably ionized gas and stars are not co-spatial in a starburst (Calzetti 1996).

The extinction derived above pertains only to the ultraviolet light within the GHRS aperture; however, the IUE spatial profile indicates that the ultraviolet light is extended, at least along P.A.=135°.45. Figure 6 shows the IUE ultraviolet light profile that was obtained by adding all the data in the dispersion direction in the wavelength range from 1250 to 1850 Å. The IUE aperture was oriented at P.A.= 135°.45. The profile shows a wing on one side that extends between 4 and 10 arcsec from the camera pixel with the highest emission. This wing could represent the ultraviolet emission from the circumnuclear region called A by GD95. We have followed the same procedure to determine the extinction for the IUE spectrum. After correcting for Galactic extinction, the spectral index of the corrected IUE spectrum is $\beta = -1.1$. This result is in agreement with that found by Heckman et al (1998), $\beta = -1.03$. The change of the slope with respect to the GHRS spectrum indicates a change of the extinction and/or of the stellar population with the aperture. The change of the extinction with the aperture could be due to the swept dust by the stellar winds and SN explosion. Using the empirical ex-

tion law from Calzetti et al (1994), we derive an internal extinction $E(B - V) = 0.3$ (2.8 mag at 1500 Å). This represents an upper limit to the reddening, because an extended population of B and A stars could contribute significantly to the ultraviolet continuum light in the IUE aperture, flattening the spectral slope, in which case the intrinsic reddening of the starburst would be lower. Thus, the IUE spectrum reveals the presence of extended star formation which could be more dusty than the nuclear burst and/or more evolved. Alternatively, the IUE aperture could pick up a large flux contribution from an older field population, that makes the slope of the spectrum flatter than expected by a hot stellar population. Note that the color excess derived depends on the extinction law used. If we use the LMC or the SMC law, the $E(B-V)$ derived is 0.2 and 0.1, respectively, instead of 0.3.

3.4. Intrinsic Luminosities and the WR/O ratio

After correcting for the total extinction, $E(B-V)=0.11$, the monochromatic luminosity at 1500 Å in the GHRS aperture is $10^{39.9} \text{ erg s}^{-1} \text{ Å}^{-1}$. Assuming that the ultraviolet flux is due to a burst of 5 Myr, and a Salpeter IMF with upper limit mass cut-off of 100 M_{\odot} , the corresponding number of O stars is about 16600. Note that an upper cut-off mass of 40 M_{\odot} gives the same result. These stars produce a photon ionizing luminosity of $7.9 \times 10^{52} \text{ s}^{-1}$. We have measured the nuclear $H\beta$ flux from the 2D data in GD95 within two different apertures of sizes that bracket the GHRS aperture size, $1.2 \times 3.3 \text{ arcsec}^2$ and $1.2 \times 2 \text{ arcsec}^2$. After correcting for the extinction derived from the Balmer decrement, the ionizing photon luminosity deduced from the $H\beta$ flux within these two apertures is $8.2 \times 10^{52} \text{ s}^{-1}$ and $6.0 \times 10^{52} \text{ s}^{-1}$, respectively. This is in very good agreement with the ionizing photon luminosity deduced from the UV continuum. However, some $H\beta$ flux could be lost due to seeing and the width of the slit. Therefore a conservative upper limit to the ionizing photon luminosity is 1.4-1.6 times the values derived above. The estimated mass of the starburst is at least $5 \times 10^6 M_{\odot}$ (integrating the IMF down to a lower mass limit of 1 M_{\odot}), and the bolometric luminosity is $5 \times 10^9 L_{\odot}$, similar to the nuclear starbursts observed in Seyfert 2 galaxies (González Delgado et al 1998b). The ionizing photon luminosity predicted by continuous star formation models is $10^{53.5} \text{ ph s}^{-1}$, a factor 4 larger

than the value deduced from the $H\beta$ flux.

We can estimate the number of WR stars from the luminosity of the HeII $\lambda 1640$ line measured within the GHRS aperture. After dereddening, and assuming the calibration given by Conti (1996; 1 WN corresponds to $6.3 \times 10^{36} \text{ erg s}^{-1}$), the line flux gives a luminosity of $10^{40.1} \text{ erg s}^{-1}$, corresponding to about 2000 WR stars. This number of WR stars gives a WR/O ratio of 0.12. The equivalent width of the HeII $\lambda 1640$ is 2.7 Å. These two numbers are compatible with the values predicted by an instantaneous burst (see Figures 2 and 10 in Schaerer & Vacca 1998). Our conclusion is that a burst 5 Myr old with a mass of $5 \times 10^6 M_{\odot}$ is able to explain the continuum and stellar UV absorption features in the central $1.74 \times 1.74 \text{ arcsec}$ of NGC 7714, with a Salpeter IMF and upper mass limit higher than 40 M_{\odot} .

The monochromatic luminosity at 1500 Å in the IUE aperture is $10^{41.25} \text{ erg s}^{-1} \text{ Å}^{-1}$, after correcting for a total reddening $E(B-V)=0.38$. This implies a bolometric luminosity of $1.1 \times 10^{11} L_{\odot}$, an ionizing photon luminosity of $2 \times 10^{54} \text{ ph s}^{-1}$ and a mass of $1.2 \times 10^8 M_{\odot}$ (assuming an age of 5 Myr), a factor 20 larger than the values derived from the GHRS aperture. The IUE bolometric luminosity is similar to the total IR luminosity, $5 \times 10^{10} L_{\odot}$, measured by IRAS and computed with the four wavelength bands as defined by Sanders & Mirabel (1997). Thus, this extended star-formation region could contribute significantly to the overall galaxy bolometric luminosity. However, these results have been derived under the assumption that the change in the slope in the IUE spectrum is due to internal extinction. If an underlying older population contributes significantly to the IUE aperture by flattening the spectrum, the derived color excess, and the mass, bolometric luminosity and the ionizing photon luminosity, represent an upper limit to the true values. The other extreme case is to assume that no internal extinction affects the IUE flux. In this case, the monochromatic luminosity at 1500 Å is $10^{40.1} \text{ erg s}^{-1} \text{ Å}^{-1}$. This implies an ionizing photon luminosity of $1.2 \times 10^{53} \text{ ph s}^{-1}$, which is a factor 2.5 lower than the rate of ionizing photons derived from the $H\alpha$ image adding the contribution of the nucleus and the region A (note that these two components fall within the IUE aperture, see Figure 1 in GD95). Thus, the change of slope is probably due to both, a change of reddening and the contribution of an underlying population.

Evidence that an underlying population contributes

to the IUE aperture comes from the CIV profile. This line is significantly more diluted in the IUE than in the GHRS spectrum (Figure 7). Thus, the IUE spectrum suggests that an underlying population contributes to its flux, and this makes the determination of the starburst properties from the IUE flux rather uncertain.

3.5. Interstellar lines and $L\alpha$ emission

The ultraviolet spectrum shows two systems of interstellar lines, one formed in the Milky Way halo and the other in NGC 7714 (see Figure 1). The most prominent lines in NGC 7714 are AlII λ 1670, FeII λ 1608, SiII λ 1527, CII λ 1335, OI+SiII λ 1302, SiII λ 1260 and SiII λ 1190. The equivalent widths of these lines are shown in Table 1. Their values are uniformly distributed between 2 and 3 Å, indicating that the lines are saturated. In the saturated part of the curve of growth the line equivalent width depends on the velocity dispersion rather than on the column density, so it can be used to constrain the kinematics of the interstellar medium (Heckman & Leitherer 1997; González Delgado et al 1998a). The equivalent width of the SiII λ 1260 implies a velocity dispersion of 160 km s⁻¹, which is consistent with the upper limit derived from the FWHM of these lines. Note that the lines are not resolved since our instrumental resolution is 3.3 Å, corresponding to a velocity dispersion of about 300 km s⁻¹. The observed equivalent width could be the result of large scale motions of the interstellar gas. This has also been observed in other starburst galaxies (Heckman & Leitherer 1997; González Delgado et al 1998a). However, in contrast to other starbursts, the ultraviolet absorption lines in NGC 7714 are not blueshifted with respect to their systemic velocity.

$L\alpha$ is observed in emission. The measured flux is 2.9×10^{-14} erg s⁻¹ cm⁻² and the equivalent width is 1.5 Å. The line shows a pronounced drop in the blue wing, due to interstellar $L\alpha$ absorption in our Galaxy and in NGC 7714 itself. This absorption shifts the peak of the emission line to the red with respect to the systemic velocity. This has also been observed in other starburst galaxies (Lequeux et al 1995; González Delgado et al 1998a; Kunth et al 1998). To correct the $L\alpha$ emission from the absorption, we have performed a multiple component fit to the observed absorption features (SiII λ 1190,1193, Galactic $L\alpha$ and $L\alpha$ in NGC 7714; we assume that $L\alpha$ in NGC 7714 is at the rest wavelength) using theoretical Voigt

profiles produced with the XVoigt software package (Mar & Bailey 1995). After dividing the observed spectrum by the fitted Voigt profiles, the $L\alpha$ flux is 2.9×10^{-13} erg s⁻¹ cm⁻² and the $L\alpha/H\beta$ ratio 2.9 (4.1 using the $H\beta$ flux measured in the central 1.2×2 arcsec²). Correcting by the reddening derived from the Balmer decrement and using the LMC extinction law, the ratio is 23 (33); close to the value predicted from the recombination theory (33, Ferland & Osterbrock 1985). We can conclude that attenuation by dust due to multiple resonant scattering by hydrogen atoms does not play an important role in NGC 7714 because the $L\alpha/H\beta$ ratio corrected for extinction is close to the recombination value.

4. Stellar content in the nuclear starburst: fitting the optical-near infrared emission line spectrum

The emission line spectrum of a starburst depends on the radiation field from the ionizing stellar cluster, and the density and chemical composition of the gas. In this section, we predict the emission line spectrum using a photoionization code that takes as input the spectral energy distribution generated by a stellar evolutionary synthesis code. This technique is applied as a second independent method to constrain the star formation history and the age of the nuclear starburst in NGC 7714. It has been previously used to study the stellar content in starbursts and giant HII regions (García-Vargas & Díaz 1994; García-Vargas, Bressan, & Díaz 1995a, 1995b; Stasińska & Leitherer 1996; García-Vargas et al 1997). The goal is to perform a test of consistency between the young stellar content derived from the ultraviolet absorption spectrum and from the optical emission lines. First, we describe the basis of the stellar evolutionary synthesis and photoionization models.

4.1. Stellar evolutionary synthesis models

The spectral energy distribution was generated by the evolutionary synthesis code developed by Leitherer and collaborators (Leitherer, Robert, & Drissen 1992). The code has been updated recently. A description of the new version will be presented elsewhere (Leitherer et al 1998, in preparation). Two important changes have been made with respect to the previous version of the code. The most recent stellar evolutionary models of the Geneva group (Schaller et al 1992; Maeder 1994), and the stellar atmospheres

grid compiled by Lejeune et al (1996) are used, instead of Maeder’s (1990) and Kurucz’s models (1992). As in the previous version of the code, we use the expanding spherical extended non-LTE models published by Schmutz et al (1992) for stars with very strong winds.

The spectral energy distribution was generated using the $0.4 Z_{\odot}$ metallicity tracks (note that the chemical abundance derived from the emission lines in NGC 7714 is close to half solar, GD95), and assuming two different star formation scenarios (instantaneous burst and continuous star formation). In both cases, a Salpeter IMF with an upper and lower mass limit cut-off of $80 M_{\odot}$ and $1 M_{\odot}$, respectively, was assumed.

4.2. Photoionization models

We take the spectral energy distribution as input to the photoionization code CLOUDY (version 90.04, Ferland 1997). CLOUDY resolves the ionization-recombination and heating-cooling balances, and predicts the ionization structure of the nebula, the temperature, and the intensities of the emission lines. We assume that the nebular gas is ionization bounded and spherically distributed around the ionizing cluster with a constant density. We assume an inner radius of 3 pc, but the outer radius is determined by the ionization front. The chemical composition of the gas is scaled to the oxygen abundance (close to half solar), except for He, S, Ne and N. The abundances and the electron density were determined from the optical emission lines as given by GD95. They are shown in Table 2. The adopted values of the solar abundance are as in Stasińska (1990), except the sulfur abundance, for which we take the S/O ratio given by Grevesse & Anders (1989). The ionizing photon luminosity is fixed to $\log(Q)=52.9 \text{ ph s}^{-1}$, as derived above independently from the Balmer recombination lines and from the ultraviolet continuum luminosity. Models are computed taking the filling factor as a free parameter, with values of 10^{-1} , 10^{-2} , 10^{-3} , 10^{-4} , and 10^{-5} . The change in the filling factor is equivalent to changing the ionization parameter U , defined as $Q/(4\pi R_s N_e c)$; where Q is the ionizing photon luminosity, N_e the electron density, c the speed of light and R_s the Strömgren radius. The average U is proportional to $(\phi^2 N_e Q)^{1/3}$, where ϕ is the filling factor.

The emission line spectrum depends on the ionizing radiation field — i.e. on the evolution of the cluster — and on the ionization parameter for a fixed

geometry, metallicity, density and the total number of ionizing photons. First, we determine the ionization parameter using the ratio $[\text{SII}]\lambda 6716+6731/\text{H}\beta$. This ratio is a good calibrator of U for continuous star formation and for burst models (Figure 8). The observed ratio $[\text{SII}]\lambda 6716+6731/\text{H}\beta=0.58$ indicates an ionization parameter of -2.9 , corresponding to a filling factor of 0.001. Then, we use the other emission lines to constrain the star formation scenario (burst or continuous star formation) and the age of the starburst. Figure 9 shows the line ratios $[\text{OIII}]\lambda 5007/\text{H}\beta$, $[\text{SIII}]\lambda 9069/\text{H}\beta$, $[\text{OII}]\lambda 3727/\text{H}\beta$, $[\text{NII}]\lambda 6584/\text{H}\beta$, $[\text{OI}]\lambda 6300/\text{H}\beta$ and $\text{HeI}\lambda 4471/\text{H}\beta$ as a function of age for continuous star formation and burst models with filling factor 0.001. Burst models predict line ratios that are in better agreement with the observed ratios than continuous star formation models. Table 3 shows the strength of the emission lines observed and the values predicted by the 4.5 Myr burst. The 4.5 Myr burst model fits well the strongest emission lines, but it does not reproduce the $[\text{OIII}]\lambda 4363$ and $[\text{OI}]\lambda 6300$ lines; the values observed are a factor of two larger than predicted. GD95 did three different estimations of the electron temperature of the nebula using the ratio of the auroral to the nebular collisionally excited lines $[\text{SIII}]$, $[\text{SII}]$ and $[\text{NII}]$ lines. The three ratios give a similar electron temperature (about 7500 K), and with this electron temperature the metallicity was derived. However, the observed $[\text{OIII}]\lambda 4363/[\text{OIII}]\lambda 5007$ ratio is larger than the expected ratio for a nebula with a electron temperature of 7500 K. This is probably a consequence of a larger contribution of the $[\text{OIII}]\lambda 4363$ line to the temperature ratio. In a nebula the presence of shocks can significantly affect the lines $[\text{OIII}]\lambda 4363$ and $[\text{OI}]\lambda 6300$ (Peimbert, Sarmiento, & Fierro 1991). Shocks are naturally expected to be present in the ionized gas surrounding a starburst with age of 5 Myr as a result of the stellar wind and the explosion of the first supernovae in the stellar cluster. At this age, the deposition rate of mechanical energy is about 10% of the ionizing luminosity. Thus, shock heating could probably account for the excess emission in $[\text{OIII}]\lambda 4363$ and $[\text{OI}]\lambda 6300$ with respect to the photoionization values.

This photoionization model predicts a Strömgren radius of 185 pc. If the nebula is radiation bounded, the radius is a function of the ionizing photon flux, the electron density and the filling factor. Then for fixed Q , N_e and Φ , the radius has to be equal to the size of the nebula. We know that the ionizing cluster

is not a point source because the ultraviolet interstellar absorption lines in the GHRS spectrum are not resolved. It is at least as extended as the size of the GHRS aperture (330×330 pc). This size is similar to the Strömgren radius predicted. Also, from the WFPC2 image (see Figure 2), we estimate that the size of the nebula is about 210 pc. Thus, the predicted size of the Strömgren radius is compatible with the estimated size of the HII nebula. This result is also consistent with the HII region being radiation bounded. Further evidence comes from the [OI] $\lambda 6300$ line. This low ionization line forms in the partially ionized zone, which does not exist in a matter bounded nebula. On the other hand, the ionizing photon flux derived from the ultraviolet continuum luminosity is very similar to that derived from the $H\beta$ luminosity, indicating again that the radiation bounded hypothesis is correct.

Thus, the conclusion is that emission line ratios can discriminate very well between the burst and continuous star formation (csf) scenario. The csf models can be excluded because they predict emission line ratios which are higher than the values observed (except for the [NII] $\lambda 6584/H\beta$). The best fit is found for a burst 4.5 Myr old. Is it reasonable that all these stars are formed in an instantaneous burst? The ultraviolet data indicate that the starburst is extended at least 1.74 arcsec (330 pc). The HST optical image shows that it may not be more extended than 400 pc (in diameter). Taking 400 pc as the diameter of the nuclear starburst and the velocity dispersion for this galaxy of 180 km s^{-1} (GD95), we derive that the crossing time within the starburst is 2.1 Myr. This time is significantly shorter than the evolutionary lifetime of a single generation of massive stars. Thus, it is dynamically possible that the nuclear starburst in NGC 7714 formed in an instantaneous burst of star-formation because the crossing-time is shorter than the duration of the starburst.

5. Discussion

5.1. X-ray and radio emission

Can the derived stellar population explain the observed X-ray luminosity and radio continuum emission? X-ray emission in normal galaxies can have several origins. As discussed by Martin & Kennicutt (1995) and Stevens & Strickland (1998), production of X-rays in starburst galaxies by AGNs, static galactic coronae, single stars, or X-ray binaries is rather unlikely to be the dominant mechanism. The most

plausible interpretation is due to powering by supernovae, with some contribution from stellar winds.

The models of Leitherer & Heckman (1995) predict a type II supernova rate of about 0.007 yr^{-1} for a bolometric luminosity of $5 \times 10^9 L_{\odot}$. If we assume that the kinetic energy released per supernova is 10^{51} erg, the mechanical luminosity released by stellar winds and supernovae is $2 \times 10^{41} \text{ erg s}^{-1}$. If thermalization occurs, this luminosity is *in principle* available to create a hot, over-pressured bubble. In practice, the sum of the thermal and kinetic energy of the bubble will be lower due to radiation losses. Hydrodynamical simulations by Thornton et al. (1998) suggest radiation losses on the order of 90%. The observed X-ray luminosity in the center of NGC 7714 is $6 \times 10^{40} \text{ erg s}^{-1}$ (W81). If interpreted as due to thermal emission from hot, shocked material, it could be accounted for by supernovae and winds, even allowing for significant radiation losses.

The observed 20 cm radio flux is 20 mJy (W81). In the standard supernova driven outflow model (e.g., Chevalier 1982; 1991) radio emission is assumed to be synchrotron radiation from electrons accelerated by shocks in the interaction zone. Models for the non-thermal component of a hot bubble are substantially more uncertain than the thermal (X-ray) prediction. Empirical data for individual local supernova remnants indicate non-thermal luminosities of about 1% the thermal value (Chevalier 1982). Assuming the 20 cm flux is purely non-thermal, and adopting a bandwidth of $\Delta\nu = 10 \text{ GHz}$, the non-thermal component in NGC 7714 has a luminosity of $3.7 \times 10^{38} \text{ erg s}^{-1}$. Remarkably, this is about 1% of the X-ray luminosity. Therefore we conclude that both the thermal and the non-thermal component of the hot, central ISM in NGC 7714 are consistent with being powered by winds and supernovae.

While simple energy considerations are instructive, more detailed hydrodynamical calculations for the behavior of a hot superbubble power by a stellar population are needed. Although still deficient in some aspects (e.g. with respect to the time dependence of the energy input), the relations discussed by Martin & Kennicutt (1995) and Stevens & Strickland (1998) provide further insight. These authors used the standard superbubble model to solve the energy and momentum equations for an adiabatic bubble. According to these models, the X-ray luminosity can be expressed in terms of the starburst luminosity and age for a given IMF. A 5 Myr old starburst with a

standard Salpeter IMF is predicted to have a ratio of the X-ray over bolometric luminosity of $\sim 10^{-3}$ (see Fig. 16 of Stevens & Strickland). Applied to NGC 7714, these models predict an X-ray luminosity of $2 \times 10^{40} \text{ erg s}^{-1}$, within a factor of 3 of the observed value. The fact that the prediction is lower than the observation might suggest a clumpy ISM. An ambient medium containing clouds or filaments can generate extra mass, and therefore extra X-ray luminosity for fixed mechanical luminosity input (Martin & Kennicutt). However, the theoretical and observational uncertainties are large enough that the data are consistent with a homogeneous medium as well.

The stellar population, as derived independently from nebular emission lines and stellar absorption lines, is capable of generating the mechanical energy input to account for the observed thermal X-ray and non-thermal radio emission as well. The associated supernova rate is 0.007 yr^{-1} . This rate is consistent with the upper limit imposed by the null result in the supernova search of Richmond, Filippenko, & Galisky (1998). No supernovae were detected in NGC 7714 during a several year long monitoring period. The non-detection implies an upper limit to the supernova rate of $< 0.1 \text{ yr}^{-1}$. Few if any supernovae should escape detection due to dust extinction since the extinction is known to be low. We can account for most of the luminosity at 1500 \AA , which traces precisely the progenitors of type II supernovae ($M \approx 20 M_{\odot}$).

The derived supernova rate is two orders of magnitude lower than that found by W81. Their estimate was based on using X-ray and radio luminosities and lifetimes of local supernova remnants as templates and scaling them to the luminosities observed in NGC 7714. In retrospect this approach has turned out to be too simple. Supernovae and supernova remnants in dense media, like in starbursts, can have rather different properties. This may be particularly relevant to the very young starburst in NGC 7714. Few red supergiants have formed at an age of 5 Myr, and most of the supernova progenitors are predicted to be WR stars. WR stars have hydrogen-free envelopes and have stellar-wind properties quite different from red supergiants. On the other hand, W81 use the truncated starburst models of Rieke et al (1980) to estimate the mass and rate of supernovae. In these models the IMF is truncated with the high mass $\leq 30 M_{\odot}$. Therefore, they have to boost the star formation rate in order to get the ionizing photons, and therefore the supernova rate became high. However,

our data are compatible with a normal IMF.

In the last few years, young compact supernovae have been studied in detail at radio wavelengths (Weiler et al, 1986, 1990, 1991, 1992; Van Dyk et al 1992, 1993a,b; Ryder et al 1993; Yin 1994). These supernova, at the peak of their emission, can have a radio luminosity which is 100 – 1000 times larger than Cas A. The presence of these supernovae and their remnants can explain the radio luminosity detected in highly luminous IRAS galaxies (Colina & Pérez-Olea, 1992; Pérez-Olea & Colina, 1995). Evidence that these compact supernova can account for the radio emission comes from 18 cm VLBI continuum imaging observations of Arp 220. The images have revealed a dozen compact radio sources, with fluxes that can be explained by compact young radio supernova (Smith et al 1998).

Assuming that the 6 cm radio emission observed by W81 is non-thermal emission emitted by the central $1.74 \times 1.74 \text{ arcsec}$, and using the models of Colina & Pérez-Olea (1995), we derive a supernova rate of 0.07 yr^{-1} , which is in agreement with our empirical upper limit determination, but still one order of magnitude higher than the rate predicted by the model which accounts for the UV luminosity. To predict a supernova rate as high as 0.07 yr^{-1} , we need a central starburst with a UV luminosity higher than $10^{39.9} \text{ erg s}^{-1} \text{ \AA}^{-1}$. Is the estimated luminosity wrong because of a wrong estimation of the intrinsic reddening derived from the UV continuum slope? If the internal reddening were $E(B - V) = 0.25$, then the UV luminosity of the starburst in the GHRS aperture would be $10^{40.7} \text{ erg s}^{-1} \text{ \AA}^{-1}$, the supernova rate 0.05 yr^{-1} , the thermal emission 4 mJy, and the non-thermal emission 6 mJy. However, by correcting the GHRS spectrum by $E(B - V) = 0.25$, the UV spectrum appears clearly over-corrected when compared with the synthetic model. From exploring the fit of the UV continuum slope, we estimate that the intrinsic reddening cannot be higher than 0.1. Correcting for this extinction, the luminosity at 1500 \AA is $10^{40.2} \text{ erg s}^{-1} \text{ \AA}^{-1}$, the mass of the starburst $1.1 \times 10^7 M_{\odot}$ and the supernova rate 0.02 yr^{-1} . In this case, we can account for just one third of the radio emission. Compact supernova remnants are also very strong X-ray sources with luminosities in the range $10^{38} - 10^{40} \text{ erg s}^{-1}$ (e.g. SN 1978K, Ryder et al 1992; SN 1986J, Bregman & Pildis 1992; SN 1993J, Schlegel 1994). SN 1988Z was detected from ROSAT HRI observations with a luminosity of $10^{41} \text{ erg s}^{-1}$ (Fabian &

Terlevich 1996). Thus, these compact supernova remnants are brighter by several orders of magnitude than the Galactic remnants (10^{35} - 10^{37} erg s $^{-1}$ range), and they can contribute significantly to the X-ray flux.

Probably even more important, a starburst nucleus is not just a scaled-up version of an individual supernova remnant. The superposition of numerous supernova explosions and the effects of stellar winds create a hot, over-pressured bubble which expands and can experience a break-out from the galaxy (Heckman 1995). The relation between the X-ray luminosity of the bubble and the properties of the stellar population, including the supernova rate, can be quite different from what is expected on the basis of individual supernova remnants (although the physics is related). The success of the simple superbubble model discussed above is encouraging. We conclude that the previously derived supernova rate of ~ 1 yr $^{-1}$ is not supported by more recent starburst models and that the current supernova rate in the nucleus of NGC 7714 is close to about 1 per century.

Incidentally, this rate is about the same as the disk-integrated rate observed in normal spirals, including the Milky Way. NGC 7714 does not have a significantly higher total supernova rate than observed in spirals with active star formation. What distinguishes NGC 7714 (and other nuclear starbursts), is the concentration of the supernova events in the nucleus. The *nuclear* supernova rate per unit surface is about three orders of magnitude higher than that of normal galaxies.

5.2. Evidence of an additional stellar population

Is there evidence for an additional stellar component younger than 30-40 Myr in the nucleus of NGC 7714? Bursts younger than 30-40 Myr will contribute to the non-thermal emission (stars more massive than $8 M_{\odot}$ explode as supernovae, and their life-time is less than 30-40 Myr). When older than 10 Myr, they will not contribute to the strength of the emission lines, but will affect the equivalent widths of the recombination emission lines. For a burst 4.5 Myr old, the equivalent width of H β is 65 Å, however, the observed value is 30 Å. Thus, the equivalent width of H β must be diluted. But we do not know whether it is diluted by a burst younger than 30-40 Myr, or by the bulge population. In the near-infrared, the spectrum shows the CaII triplet in absorption. The strength of these lines is dependent on both metallic-

ity and gravity (Díaz, Terlevich, & Terlevich 1989). At solar metallicity, these lines are very strong in starbursts if the near-infrared light is dominated by red supergiant stars. Population synthesis models of the two strongest absorption lines (CaII $\lambda 8542$ and CaII $\lambda 8562$) for half solar metallicity predict an equivalent width for the two lines of 4-5 Å for burst younger than 40 Myr (García-Vargas et al 1998). The observed value is 4.5 Å (GD95), in agreement with the prediction of the models. However, the same models predict an equivalent width somewhat larger than 5 Å for a burst older than 100 Myr. Thus, even though the strength of the CaII triplet is compatible with a burst younger than 40 Myr, we cannot exclude that the lines could be dominated by red giant instead of red supergiant stars. Thus, the equivalent width of H β and the strength of the CaII triplet show evidence that an underlying population contributes to the central 1.7×1.7 arcsec spectrum of NGC 7714. Further evidence comes from the NIR spectrum. We will present a full analysis of the UV-optical-NIR continuum in paper II (Goldader et al 1998, in preparation).

6. Summary and conclusions

The main goal of this work is to constrain the most recent star formation history in the central 300 pc of NGC 7714. To achieve this goal, we observed the nucleus of NGC 7714 from the UV to the near infrared. Consistent with previous observations, our data show that NGC 7714 exhibits the spectral dichotomy typically observed in starburst galaxies. The ultraviolet spectrum is dominated by absorption features formed in the interstellar medium and stellar winds, while the optical spectrum is dominated by emission lines formed in the photoionized interstellar medium. We constrain the most recent star formation history in the nucleus of NGC 7714 by applying two different techniques, one based on the ultraviolet spectrum, and the other on the optical to near infrared emission line spectrum.

Evolutionary synthesis line profiles of the CIV and SiIV wind lines are used to constrain the duration of the starburst, the age of the stellar population, and the IMF parameters (slope and upper limit). We find that the profiles of the wind lines are compatible with a single burst, an age of 5 Myr and a Salpeter IMF with upper mass cut-off higher than $40 M_{\odot}$. Arguments of causality suggest that is dynamically pos-

sible that the nuclear starburst formed an instantaneous burst since the dynamical crossing time within the starburst is lower than the evolutionary life time of massive stars. Evolutionary synthesis models coupled to the photoionization code CLOUDY are also used to generate the emission line spectrum. Continuum star formation models are not consistent with the strength of the emission line ratios. The best fit to the emission lines is found for a 4.5 Myr burst model. From the ultraviolet continuum luminosity we derive a mass of the starburst of $5\text{--}11 \times 10^6 M_{\odot}$ (note that this probably a lower limit to the mass of the starburst because it has been derived from the UV continuum luminosity) and a bolometric luminosity of $5\text{--}10 \times 10^9 L_{\odot}$, assuming stars down to $1 M_{\odot}$ are formed. Very little extinction is associated with this nuclear starburst. WR features at ultraviolet (HeII $\lambda 1640$) and optical (HeII $\lambda 4686$) wavelengths are detected. Their luminosities imply a WR/O ratio of ~ 0.1 , which is also compatible with the predicted values from the burst models.

This model predicts a supernova rate of $0.007\text{--}0.02 \text{ yr}^{-1}$, consistent with the rate derived from the radio and the X-ray luminosities, 0.05 yr^{-1} (if the emission accounts for the contribution of radio and X ray compact supernova). This rate is in agreement with an upper limit of 0.1 yr^{-1} based on the non-detection of supernova events in the past several years. This supernova rate is two order of magnitude lower than previously suggested. The supernova rate in the NGC 7714 nucleus is similar to disk-integrated rates in normal spiral galaxies.

Acknowledgments

We thank Gary Ferland for kindly making his code available, and David Mar for providing his XVoigt software package. M.L. García-Vargas is grateful to the Space Telescope Science Institute for the kind support provided during part of this work. We have benefited from stimulating and helpful discussions with Itziar Aretxaga, Miguel Cerviño, Luis Colina, Ariane Lançon, Enrique Pérez, Daniel Schaerer and Kim Weaver. We thank the staff at STScI for their help in obtaining the data presented in this paper and to Antonella Nota for her help at the beginning of this project. This work was supported by HST GO-06672.01-95A from the Space Telescope Science Institute, which is operated by the Association of Universities for Research in Astronomy, Inc., under NASA contract NAS5-26555.

REFERENCES

- Arp, H. 1966, *Atlas of peculiar galaxies*, CalTech, Pasadena, California
- Bernlöhr, K. 1993, *A&A*, 268, 25
- Bohlin, R.C. 1975, *ApJ*, 200, 402
- Bregman, J.N., & Pildis, R.A. 1992, *ApJ*, 398, L107
- Bruzual, A.G., & Charlot, S. 1993, *ApJ*, 405, 538
- Calzetti, D. 1997, *AJ*, 113, 162
- Calzetti, D. 1996, *From stars to galaxies: the impact of stellar physics on galaxy evolution*, ed. C. Leitherer, U. Fritze-von Alvensleben & J. Huchra (San Francisco: ASP), 446
- Calzetti, D., Kinney, A.L., & Storchi-Bergmann, T. 1994, *ApJ*, 429, 582
- Castor, J.I., Abbot, D.C., & Klein, R.I. 1975, *ApJ*, 195, 157
- Chevalier, R.A. 1982, *ApJ*, 259, 302
- Chevalier, R.A. 1991, in *Massive Stars in Starbursts*, ed. C. Leitherer, N. Walborn, T. Heckman, & C. Norman (Cambridge: CUP), p. 169
- Colina, L., & Pérez-Olea, D. 1992, *MNRAS*, 259, 709
- Conti, P.S. 1996, in *Interplay between massive star formation, the ISM and galaxy evolution*, ed. Kunth, D., Guiderdoni, B., Heydari-Malayeri, M., & Thuan, T.X., Gif-sur-Yvette: Editions Frontières, p. 37.
- Conti, P.S., Leitherer, C., & Vacca, W.D. 1996, *ApJ*, 461, L87
- de Vaucouleurs, G., de Vaucouleurs, A., Corwin, H.G., Buta, R.J., Paturel, G., Fouqué, P. 1991, *Third Reference Catalogue of Bright Galaxies*, (New York: Springer-Verlag)
- Díaz, A., Terlevich, E., & Terlevich, R. 1989, *MNRAS*, 239, 325
- Fabian, A.C., & Terlevich, R. 1996, *MNRAS*, 280, L5
- Fanelli, M., O'Connell, R., & Thuan, T., 1988, *ApJ*, 334, 665
- Ferland, G.J. 1997, *Hazy*, a Brief Introduction to CLOUDY, University of Kentucky, Department of Physics and Astronomy Internal Report
- Ferland, G.J., & Osterbrock, D.E. 1985, *ApJ*, 289, 105
- García-Vargas, M.L., & Díaz, A.I. 1994, *ApJS*, 91, 553
- García-Vargas, M.L., Bressan, A., & Díaz, A.I. 1995a, *A&AS*, 112, 13
- 1995b, *A&AS*, 112, 35
- García-Vargas, M.L., González-Delgado, R.M., Pérez, E., Alloin, D., Díaz, A.I., & Terlevich, E. 1997, *ApJ*, 478, 112
- García-Vargas, M.L., Mollá, M., & Bressan, A. 1998, *A&AS*, 130, 513
- González Delgado, R.M., Heckman, T., Leitherer, C., Meurer, G., Krolik, J., Wilson, A.S., Kinney, A.L., & Koratkar, A. 1998b, *ApJ*, 505, in press
- González Delgado, R.M., Leitherer, C., & Heckman, T. 1997, *ApJ*, 489, 601
- González Delgado, R.M., Leitherer, C., Heckman, T., Ferguson, H.C., Lowenthal, J.D., & Robert, C. 1998a, *ApJ*, 495, 698
- González-Delgado, R.M., Pérez, E., Díaz, A.I., García-Vargas, M.L., Terlevich, E., & Vílchez, J.M. 1995, *ApJ*, 439, 604, (GD95)
- Grevesse, N., & Anders, E. 1989, *Cosmic Abundances of Matter*, *AIP Conference Proc.*, ed. C.J.. Waddington, New York, p. 183,
- Groenewegen, M.A.T., Lamers, H.J.G.L.M., & Pauldrach, A.W.A. 1989, *A&A*, 221, 78
- Heckman, T.M. 1995, in *Interplay between massive star formation, the ISM and galaxy evolution*, ed. Kunth, D., Guiderdoni, B., Heydari-Malayeri, M., & Thuan, T.X., Gif-sur-Yvette: Editions Frontières, p. 159
- Heckman, T.M. 1998, in *Star Formation Near and Far*, ed. S.S. Holt & L.G. Mundy (San Francisco: ASP), in press
- Heckman, T.M., González-Delgado, R.M., Leitherer, C., Meurer, G.R., Krolik, J., Wilson, A., Kinney, A.L., & Koratkar, A. 1997, *ApJ*, 482, 114

- Heckman, T.M., & Leitherer, C. 1997, *AJ*, 114, 69
- Heckman, T.M., Robert, C., Leitherer, C., Garnett, D., & van der Rydt, F., 1998, *ApJ*, 503, 646
- Kinney, A. L., Bohlin, R. C., Calzetti, D., Panagia, N., & Wyse, R. 1993, *ApJS*, 86, 5
- Kunth, D., Mas-Hesse, J.M., Terlevich, E., & Terlevich, R. 1998, *A&A*, in press
- Kurucz, R. L. 1992, *The stellar Populations of Galaxies*, in IAU Symp. 149, ed. B. Barbuy & A. Renzini, Dordrecht: Kluwer, p. 225
- Leitherer, C. 1996, *From stars to galaxies: the impact of stellar physics on galaxy evolution*, ed. C. Leitherer, U. Fritze-von Alvensleben & J. Huchra (San Francisco: ASP), 373
- Leitherer, C. 1997, *The ultraviolet universe at low and high redshift: Probing the progress of galaxy evolution*, ed. W. H. Waller, M. N. Fanelli, J.E. Hollis & A. C. Danks, AIP Conference proceedings 408, 119
- Leitherer, C., & Heckman, T.M. 1995, *ApJS*, 96, 9
- Leitherer, C., Robert, C., & Drissen, L. 1992, *ApJ*, 401, 596
- Leitherer, C., Robert, C., & Heckman, T. M. 1995, *ApJS*, 99, 173
- Leitherer, C., Vacca, W.D., Conti, P.S., Filippenko, A.V., Robert, C., & Sargent W.L.W. 1996, *ApJ*, 465, 717
- Lejeune, T., Cuisinier, F., & Buser, R. 1996, in *From stars to galaxies: the impact of stellar physics on galaxy evolution*, ed. C. Leitherer, U. Fritze-von Alvensleben & J. Huchra, (San Francisco ASP), p. 94
- Lequeux, J., Kunth, D., Mas-Hesse, J.M., & Sargent, W.L. 1995, *A&A*, 301, 18
- Lucy, L. B., & Solomon, P. M. 1970, *ApJ*, 159, 879
- Maeder, A. 1990, *A&AS*, 84, 139
- 1994, *A&A*, 287, 803
- Mar, D.P., & Bailey, G. 1995, *Proc. ASA*, 12, 239
- Martin, C.L., & Kenicutt, R.C. 1995, *ApJ*, 447, 171
- Mas-Hesse, J.M., & Kunth, D. 1991, *A&AS*, 88, 317
- Mirabel, I.F., & Wilson, A. 1989, *ApJ*, 277, 92
- Morton, D. C. 1967, *ApJ*, 147, 1017
- Peimbert, M., Sarmiento, A., & Fierro, J. 1991, *PASP*, 103, 815
- Pérez-Olea, D., & Colina, L. 1995, *MNRAS*, 277, 857
- Prinja, R. K., Barlow, M. J., & Howarth, I. D. 1990, *ApJ*, 361, 607
- Richmond, M.W., Filippenko, A.V., & Galisky, J. 1998, *PASP*, 110, 553
- Rieke, G.H., Lebofsky, M.J., Thompson, R.I., Low, F.J., Tokunaga, A.T. 1980, *ApJ*, 238, 24
- Robert, C., Leitherer, C., & Heckman, T. M. 1993, *ApJ*, 418, 749
- Ryder, S., Staveley-Smith, L., Dopita, M., Petre, R., Colbert, E., Malin, D., & Schlegel, E. 1993, *ApJ*, 416, 167
- Sanders, D.B., & Mirabel, I.F. 1997, *ARAA*, 34, 749
- Schaerer, D., & Vacca, W.D. 1998, *ApJ*, 497, 618
- Schaller, G., Schaerer, D., Meynet, G., & Maeder, A. 1992, *A&AS*, 96, 269
- Schechter, P. 1980, *AJ*, 85, 801
- Schlegel, E.M. 1994, in *The Soft X-ray Cosmos*, ed. E.M. Schlegel & R. Petre, New York: AIP, 195
- Schmutz, W., Leitherer, C., & Gruenwald, R.B. 1992, *PASP*, 104, 1164
- Smith, B.J., Struck, C., & Pogge, R. 1997, *ApJ*, 483, 754
- Smith, H. E., Lonsdale, C.J., Lonsdale, C.J., & Diamond, P.J. 1998, *ApJ*, 493, L17
- Stark, A., Gammie, C., Wilson, R., Bally, J., Linke, R., Heiles, C., & Hurwitz, M. 1992, *ApJS*, 79, 77
- Stasińska, G. 1990, *A&AS*, 83, 501
- Stasińska, G., & Leitherer, C. 1996, *ApJS*, 107, 661
- Stevens, I.R., & Strickland, D.K. 1998, *MNRAS*, 294, 523

- van Breugel, W., Filippenko, A.V., Heckman, T., & Miley, G. 1985, ApJ, 293, 83
- Van Dyk, S.D., Weiler, K.W., Sramek, R.A., & Panagia, N. 1992, ApJ, 396, 195
- Van Dyk, S.D., Weiler, K.W., Sramek, R.A., & Panagia, N. 1993b, ApJ, 419, L69
- Van Dyk, S.D., Sramek, R.A., Weiler, K.W., & Panagia, N. 1993a, ApJ, 409, 162
- Vorontsov-Velyaminov, B.A. 1977, A&AS, 28, 1
- Walborn, N. R., Bohlin, J. N., & Panek, R. J. 1985 *International Ultraviolet Explorer Atlas of O-Type Spectra from 1200 to 1900 Å (NASA RP-1155)*
- Walborn, N. R., Parker, J., & Nichols, J.S. 1995, *International Ultraviolet Explorer Atlas of B-type Spectra from 1200 to 1900 Å (NASA RP-1363)*
- Weedman, D.W. 1983, ApJ, 266, 479
- Weedman, D.W, Feldman, F.R., Balzano, F.R., Ramsey, L.W., Sramek, R.A., & Wu, C.C. 1981, ApJ, 248, 105
- Weiler, K.W., Panagia, N., & Sramek, R.A. 1990, ApJ, 364, 611
- Weiler, K.W., Sramek, R.A., Panagia, N., Van der Hulst, J.M., & Salvati, M. 1986, ApJ, 301, 790
- Weiler, K.W., Van Dyk, S.D., Panagia, N., & Sramek, R.A. 1992, ApJ, 398, 248
- Weiler, K.W., Van Dyk, S.D., Panagia, N, Sramek, R.A., & Discenna, J. L. 1991, ApJ, 380, 161
- Yin, Q.F. 1994, ApJ, 420, 152

TABLE 1
EQUIVALENT WIDTH (\AA) OF THE ABSORPTION AND EMISSION FEATURES^a

Line	type	Ew (\AA)
NV $\lambda 1240$	W	2.8
NV $\lambda 1240$	W	-1.2
SiII $\lambda 1260$	IS	1.7
OI+SiII $\lambda 1300$	IS	3.1
CII $\lambda 1335$	IS	2.8
SiIV $\lambda 1400$	W+IS	6.4
SiIV $\lambda 1400$	W	-0.2
SiIII $\lambda 1417$	Ph	0.6
CIII $\lambda 1428$	Ph	0.5
SV $\lambda 1501$	Ph	0.8
SiII $\lambda 1526$	IS	2.1
CIV $\lambda 1550$	W+IS	9.4
CIV $\lambda 1550$	W	-0.9
FeII $\lambda 1608$	IS	1.8
HeII $\lambda 1640$	W	-1.6

^aIS means Interstellar, W wind, and Ph Photospheric line. Negative values are lines in emission.

TABLE 2
INPUT PARAMETERS FOR CLOUDY ^a

parameter	value
$\log N_e$	2.75
$12+\log \text{O/H}$	8.53
$\log \text{He/H}$	-1.00
$\log \text{S/H}$	-5.05
$\log \text{Ne/H}$	-4.30
$\log \text{N/H}$	-4.15

^aThe electron density and metallicity are from GD95, and they were derived from the optical emission lines.

TABLE 3
LINE RATIO OF THE EMISSION LINES WITH RESPECT TO $H\beta$ ^a

Line	observed	model
[OII] $\lambda 3727$	1.97	2.13
[OIII] $\lambda 4363$	0.01	0.005
HeI $\lambda 4471$	0.037	0.04
[OIII] $\lambda 5007$	1.59	1.83
HeI $\lambda 5876$	0.12	0.12
[SIII] $\lambda 6312$	0.007	0.01
[OI] $\lambda 6300$	0.043	0.022
[NII] $\lambda 6584$	1.22	1.37
[SII] $\lambda 6716$	0.29	0.32
[SII] $\lambda 6732$	0.28	0.32
[SIII] $\lambda 9069$	0.27	0.32

^aThe observed line ratios are from GD95 corrected for reddening with $C(H\beta)=0.3$. The line ratios are predicted using the spectral energy distribution of the 4.5 Myr burst model, assuming a Salpeter IMF and $M_{\text{up}} = 80 M_{\odot}$, as the ionizing radiation field into CLOUDY.

Fig. 1.— The 1.74×1.74 arcsec² GHRS spectrum of the nucleus of NGC 7714 (in the rest frame of NGC 7714 wavelength). The most important wind, photospheric and interstellar absorption lines are labelled. The interstellar absorption lines formed in the halo of our Galaxy are also labeled as Gal.

Fig. 2.— The WFPC2 F606W image. The orientation is North up and East to the left. The scale is 0.046 arcsec/pix. (a) The image shows the morphological characteristics of almost the whole galaxy. (b) The central 2.5×2.5 arcsec². The nucleus is clearly extended, and resolved into several knots.

Fig. 3.— χ^2 parameter of the fits to the profile of SiIV for burst models (a,b), and for the continuous star formation models (c,d) with different M_{up} (a,c) and IMF slope (b,d). The size of the bubble is proportional to χ^2 , with a larger size indicating a worse fit. The scale in the small boxes indicates the value of χ^2 .

Fig. 4.— The observed profiles (dashed line) of CIV (a) and SiIV (b) and the 5 Myr burst model (thick line), assuming a Salpeter IMF and $M_{up} = 100 M_{\odot}$.

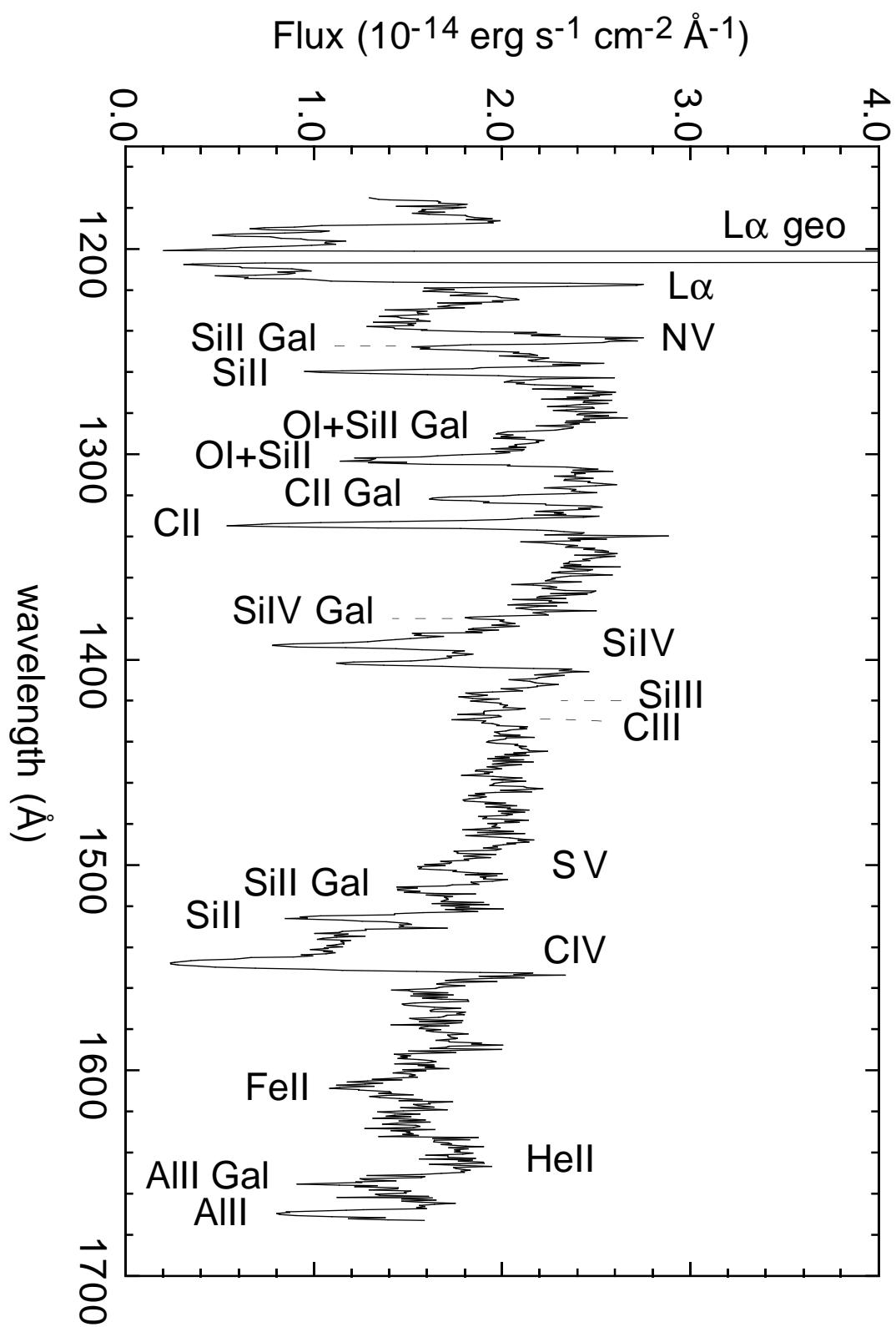
Fig. 5.— The GHRS spectrum dereddened by $E(B-V)=0.08$ using the MW extinction law, and by $E(B-V)=0.03$ using the Calzetti et al (1994) extinction law, and the synthetic 5 Myr burst model (in relative units). The IMF slope is Salpeter and $M_{up} = 100 M_{\odot}$.

Fig. 6.— The IUE intensity profile perpendicular to the dispersion direction integrating from 1250 to 1850 Å. The zero in the X-axis is the IUE camera pixel with highest ultraviolet emission. The bump between 4 and 9 arcsec could be the emission associated with the circumnuclear region called A in GD95.

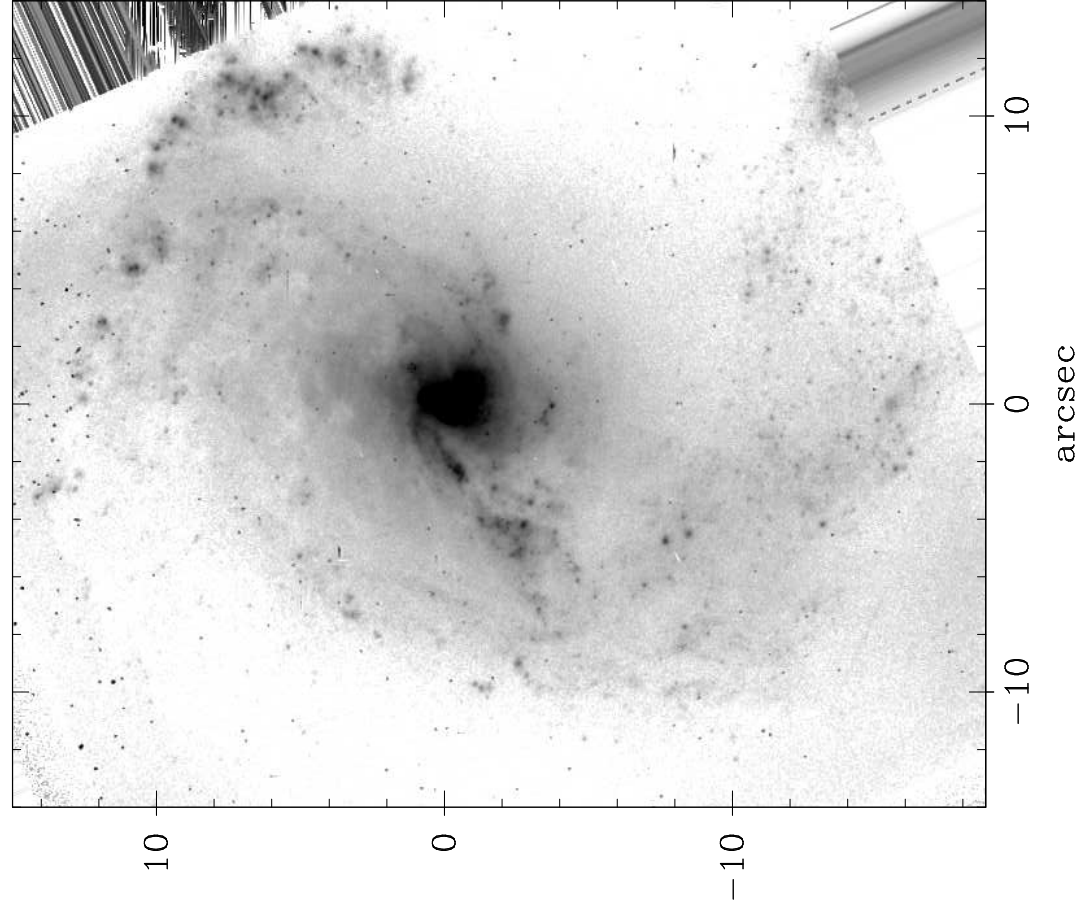
Fig. 7.— The GHRS (thick line) spectrum rebinned to the resolution of the IUE spectrum (thin line). The GHRS flux at 1500 Å is also scaled to match the IUE flux. The spectra are corrected only by Galactic extinction.

Fig. 8.— Predicted emission line ratio $[SII]\lambda 6716+6732/H\beta$ as a function of the average ionization parameter generated with CLOUDY, taking as input the spectral energy distribution from the evolution of a burst (open symbols) and continuous star forming regimes (full symbols). The observed value is indicated by a horizontal line. See text for details.

Fig. 9.— Predicted emission line ratios as a function of age. The filling factor is 0.001. The observed values are indicated by a horizontal line. These ratios are compatible with a burst 4.5 Myr old, and they exclude the continuous star formation models.



NGC 7714 – HST



NGC 7714 – HST

